ONCOIMMUNOLOGY
2025, VOL. 14, NO. 1, 2504244
https://doi.org/10.1080/2162402X.2025.2504244

Taylor & Francis
Taylor & Francis Group

ORIGINAL RESEARCH

Gasdermin E links tumor cell-intrinsic nucleic acid signaling to proinflammatory cell death for successful checkpoint inhibitor cancer immunotherapy

Stefan Enssle[a,b], Anna Sax[a,b], Peter May[a,b], Nadia El Khawanky[a,b], Nardine Soliman[a,b], Markus Perl[c], Julius C. Enssle[d], Karsten Krey[e], Jürgen Ruland[b,f,g], Andreas Pichlmair[b,e,h], Florian Bassermann[a,b,g], Hendrik Poeck[c,i,j], and Simon Heidegger[a,b*]

[a]Department of Medicine III, TUM School of Medicine and Health, Technical University of Munich, Munich, Germany; [b]Centerfor Translational Cancer Research (TranslaTUM), TUM School of Medicine and Health, Technical University of Munich, Munich, Germany; [c]Department of Internal Medicine III, University Hospital Regensburg, Regensburg, Germany; [d]Department of Medicine II, Hematology/Oncology, University Hospital Frankfurt, Goethe University, Frankfurt, Germany; [e]Institute of Virology, TUM School of Medicine and Health, Technical University of Munich, Munich, Germany; [f]Institute of Clinical Chemistry and Pathobiochemistry, TUM School of Medicine and Health, Technical University of Munich, Munich, Germany; [g]German Cancer Consortium (DKTK), Partner-site Munich and German Cancer Research Center (DKFZ), Heidelberg, Germany; [h]German Center for Infection Research (DZIF), Partner Site Munich, Munich, Germany; [i]Leibniz Institute for Immunotherapy (LIT), Regensburg, Germany; [j]Center for immunomedicine intransplantation and oncology (CITO), Regensburg, Germany

ABSTRACT

Durable clinical responses to immune checkpoint inhibitors (ICI) are limited to a minority of patients, and molecular pathways that modulate their efficacy remain incompletely defined. We have recently shown that activation of the innate RNA-sensing receptor RIG-I and associated apoptotic tumor cell death can facilitate tumor immunosurveillance and -therapy, but the mechanism that drives its immunogenicity remained unclear. We here show that intratumoral activity of the pore-forming protein gasdermin E (GSDME) links active RIG-I signaling and apoptotic cell death in tumor cells to inflammatory pyroptosis. Activation of tumor-intrinsic RIG-I triggered cleavage of GSDME, pore formation, loss of cell membrane integrity and leakage of cytosolic components from dying tumor cells. Tumor antigen cross-presentation by dendritic cells and subsequent expansion of cytotoxic T cells strongly relied on tumor-intrinsic GSDME activity. In preclinical murine cancer models, defective GSDME signaling rendered tumors resistant to ICI therapy. Epigenetic reprogramming with upregulation of *Gdsme* enhanced the susceptibility of tumor cells to inflammatory cell death and immunotherapy. In humans, transcriptome analysis of melanoma samples showed strong correlation between genetic activity of the RIG-I and pyroptosis pathways. In melanoma patients, high transcriptional activity of a pyroptosis gene set was associated with prolonged survival and beneficial response to ICI therapy. In summary, our data show that GSDME links RIG-I and apoptotic signaling to inflammatory cell death, thereby driving its immunogenicity and responsiveness to ICI. A deeper understanding of these pathways may allow for the development of novel combined modality approaches to improve ICI treatment responses in cancer patients.

ARTICLE HISTORY
Received 22 November 2024
Revised 5 May 2025
Accepted 6 May 2025

KEYWORDS
Cancer immunotherapy; immune checkpoint inhibitors; cancer resistance mechanism; immunogenic cell death; programmed cell death; apoptosis; pryroptosis; Gasdermin E; RIG-I

Introduction

Immunotherapy has dramatically changed the landscape of cancer treatment. Herein, monoclonal antibodies targeting the checkpoints cytotoxic T lymphocyte-associated protein 4 (CTLA-4) or programmed cell death protein 1 (PD-1) have yielded impressive clinical responses in various cancer entities.[1] Dual immune checkpoint inhibition (ICI) of CTLA-4 and PD-1 in the treatment of patients with metastatic malignant melanoma has achieved an overall survival of around 50% at a six-year follow-up.[2] However, while some patients experience long-term disease control and possibly cure, most cancer patients will either not respond to ICI therapy or relapse after initial treatment benefit.[3] These inter-individual differences in treatment response remain a major clinical challenge. The underlying molecular mechanisms are poorly understood but comprise both endogenous and exogenous factors, including tumor mutational burden, a T cell-inflamed tumor microenvironment (TME), or the composition of gut microbiota.[4] Generally, ICI therapies are considered to reinvigorate T-cell responses against tumor cells. However, in many patients, these therapies fail, as the initial development of spontaneous immune responses is often compromised by the immunosuppressive tumor milieu or insufficient levels of tumor antigen to reach the threshold for T-cell recognition. A prerequisite for initiating tumor-specific adaptive T-cell immune responses is that specialized antigen-presenting cells – particularly dendritic cells (DCs) – take up, process, and present tumor-associated antigens to cytotoxic T cells. Such cross-priming of tumor-specific T cells has been shown to be dependent on DC maturation mediated by type I IFN (IFN-I).[5] The tumor

CONTACT Simon Heidegger simon.heidegger@tum.de Department of Medicine III, TUM School of Medicine and Health, Technical University of Munich, Ismaningerstr. 22, 81675, Munich, Germany

*Current affiliation: Early Clinical Development, Oncology, Genentech, South San Francisco, CA, USA.

Supplemental data for this article can be accessed online at https://doi.org/10.1080/2162402X.2025.2504244

microenvironment often lacks proinflammatory signals, resulting in suboptimal DC activation.

We and others have shown previously that tumor cell-intrinsic activity of the RNA sensor RIG-I (retinoic acid-inducible gene I) is critical for responsiveness to ICI therapy.[6] RIG-I is a cytosolic receptor that primarily detects double-stranded 5′–triphosphate RNA (3pRNA) from both cell-intrinsic and extrinsic sources. Upon ligand binding, RIG-I recruits the adaptor protein MAVS (mitochondrial antiviral signaling protein) to induce IFN-I signaling, inflammasome activation, and potentially regulated cell death. The exact nature of endogenous RIG-I-activating RNA ligands remains unclear. However, therapeutic targeting of RIG-I has demonstrated strong antitumor effects mediated via IFN-I production by host immune cells and simultaneous induction of regulated cell death in malignant cells. Tumor cell-intrinsic RIG-I signaling was found to trigger a form of caspase-3-mediated apoptotic tumor cell death.[7–9] In mice, the development of an antitumor T-cell response and subsequent regression of tumors in response to checkpoint inhibitor treatment was critically dependent on the active RIG-I/caspase-3 axis in tumor cells.[6] However, the molecular components that drive the immunogenicity of such RIG-induced apoptotic tumor cell death and link it to subsequent checkpoint inhibitor-augmented antitumor immunity remain unclear.

Several recent studies have implicated that the family of gasdermins and particularly its member gasdermin E (GSDME) may play an important role in the transition from apoptosis to secondary inflammatory cell death in the form of pyroptosis.[10] Once cleaved from the inhibitory C-terminal domain by different proteases, the N-terminal domain of gasdermins harbors intrinsic pore-forming and pyroptosis-inducing capacity.[11] Different forms of immunogenic cell death are characterized by the spatiotemporally defined release of proinflammatory factors called danger-associated molecular patterns (DAMPs). DAMPs comprise both constitutively present cellular components, only released upon cell membrane disintegration, as well as factors that are *de novo* synthesized, induced by pro-inflammatory transcription factors in dying cells.[12] DAMPs that have been associated with inflammatory cell death include exposure of calreticulin on the cell surface as well as release of ATP and HMGB1.[13] GSDME has been shown – under certain circumstances – to be cleaved by the apoptosis executioner caspase-3, inducing pyroptosis in response to tumor necrosis factor (TNF) or chemotherapy.[14,15] GSDME has been suggested to act as a tumor suppressor gene,[16–21] and loss of *Gsdme* in murine tumors was found to be associated with reduced immunosurveillance.[21] However, the role of GSDMs in the treatment efficacy of immunotherapies, including checkpoint inhibitors as well as cytotoxic regimens, is poorly understood.

We here show that tumor cell-intrinsic RIG-I signaling induces cleavage of caspase-3 and GSDME, which links proapoptotic signaling to immunogenic cell death. Defects in the RIGI/caspase-3/GSDME axis in tumor cells are a cancer resistance mechanism to ICI therapy.

Material and methods

Mice

Female C57BL/6J and BALB/c mice were purchased from Janvier. Mice were at least six weeks of age at the onset of experiments and were maintained in specific pathogen-free conditions on a 12-h light – dark cycle and a constant temperature of 24°C. Animal studies were approved by the local regulatory agency (Regierung von Oberbayern, Munich, Germany, application ID ROB-55.2-2532.Vet_02-19-159).

Media and reagents

DMEM medium (Sigma Life Science) was supplemented with 10% (vol/vol) FCS, 100 U/ml penicillin and 100 µg/ml streptomycin (all Gibco). RPMI-1640 medium (Sigma Life Science) was supplemented with 10% (vol/vol) FCS, 2 mM L-glutamine, 100 U/ml penicillin, 100 µg/ml streptomycin and 50 µM 2-Mercaptoethanol (all Gibco). Advanced DMEM/F12 medium (Gibco) was supplemented with 10% (vol/vol) FCS, 2 mM L-glutamine, 100 U/ml penicillin, 100 µg/ml streptomycin and Minimum Essential Medium Non-Essential Amino Acids (MEM NEAA) (all Gibco). VLE RPMI medium (Bio&Sell) was supplemented with 10% (vol/vol) FCS, 100 U/ml penicillin, 100 µg/ml streptomycin (both Gibco) and 20 ng/ml GM-CSF (Peprotech). OptiMEM reduced serum medium was from Invitrogen. Double-stranded *in vitro*-transcribed 3pRNA (sense, 5′- UCA AAC AGU CCU CGC AUG CCU AUA GUG AGU CG −3′) was generated as described.[9] Cisplatin (Hexal) and Azacytidine (Zentiva Pharma) were obtained via the hospital pharmacy of Klinikum rechts der Isar at Technical University of Munich.

Cell lines and CRISPR-Cas9-mediated genome editing

The B16 murine melanoma cell line expressing full-length chicken ovalbumin (here referred to as B16.OVA) was cultured in complete DMEM medium, CT26 cells were cultured in complete RPMI 1640 medium. YUMMER1.7 cells were cultured in complete Advanced DMEM/F12 medium. Genetic deletion of *Gsdme* was conducted by electroporation of CRISPR/Cas9 ribonucleoprotein complexes (RNPs) into the cells. Two guide RNAs (gRNA) were used to obtain high knockout efficiency. The specific gRNAs were designed for high on-target and low off-target activity using the CRISPR Guide RNA Design Tool from Benchling and CHOPCHOP tool. First, Alt-R CRISPR-Cas9 crRNA and tracrRNA (both Integrated DNA Technologies) were annealed to gRNAs. Then, CRISPR/Cas9 RNPs, consisting of gRNAs and either TrueCut Cas9 Protein v2 (Invitrogen) or Cas9-GFP (Sigma-Aldrich), were electroporated into cells using the 4D-Nucleofector X Unit (Lonza). For B16.OVA, gene-edited cells were enriched by FACS for GFP^+ events to generate a polycloncal B16.OVA $Gsdme^{-/-}$ cell line. For CT26, 4 single gene-deficient clones were pooled to generate an oligoclonal CT26 $Gsdme^{-/-}$ cell line. Gene deficiency was identified by immunoblotting, sequencing, and functional assays. Guide RNA target sequences are listed in the Supplementary Material and Methods section.

In vitro tumor cell death assays

For *in vitro* transfection, 3pRNA was complexed with Lipofectamine 3000 and P3000 reagent (Invitrogen) in Opti-MEM (Invitrogen), and tumor cells were cultured in the presence of complexed 3pRNA (3 µg/ml) for 24 to 48 hours, if not stated otherwise. B16.OVA, CT26 and YUMMER1.7 tumor cells were cultured, if indicated, with 40 µg/ml, 20 µg/ml and 5 µg/ml cisplatin, respectively and B16.OVA melanoma cells were pretreated, if indicated, with 5-Azacytidine (5 µM). Induction of cell death was assessed by staining with Annexin V (Biolegend) and Propidium Iodide Solution (Biolegend) in Annexin V Binding Buffer 10× (eBioscience) and subsequently analyzed via Flow Cytometry. Release of LDH into the Supernatant as an indicator of loss of cell membrane integrity was measured with the CytoTox 96 Non-Radioactive Cytotoxicity Assay (Promega) according to the manufacturer ´s protocol and calculated as a percentage of LDH released into the supernatant of total LDH from the cell lysate. For Propidium Iodide (PI) uptake kinetics, 1 µg/ml PI and treatments as indicated were added to tumor cell cultures before live cell imaging with an Incucyte S3 or SX5Live-Cell Analysis System (both Sartorius). Images were acquired every two or three hours at 4× magnification and were subsequently analyzed with the Incucyte Cell-by-Cell Analysis Software (Sartorius). The percentage of PI^+ cells with thresholding in an object-wise manner was calculated by the following formula: (% red confluence/% phase confluence) x 100.

Microscopy

Images were acquired with a Leica DMi1 Microscope, Leica MC170 hD Microscope Camera and Leica Acquire Software Version 3.4.7 (Leica Microsystems GmbH) and were later analyzed with ImageJ Version 1.53a (Wayne Rasband, National Institutes of Health, USA).

Immunoblotting

Tumor cell proteins were extracted using the radioimmunoprecipitation assay (RIPA) buffer (Invitrogen), including a complete protease inhibitor cocktail (Roche) during an incubation time of 30 min on ice. Protein yield was measured by BCA assay (Thermo Fischer Scientific) according to the manufacturer's protocol. Lysates were mixed with the kit reagents and incubated for 30 min at 37 °C in the dark. Absorbance was measured at or near 562 nm on a microplate reader (Promega GloMax Discover Microplate Reader). Protein separation by SDS-PAGE was done on 12% polyacrylamide gels (NuPAGE Novex 12% Bis-Tris Gels, Invitrogen) for 20 min at 100 V followed by 80–100 min at 130 V. Proteins were blotted to a nitrocellulose blotting membrane (Thermo Scientific) for 120 min at 0.3 A and membranes were subsequently blocked for 60 min in 5% milk (Sigma-Adlrich) in 1× TBST (tris-buffered saline and Tween 20, Thermo Scientific). After incubation with primary antibodies (Supplementary Material and Methods section) in blocking buffer overnight at 4 °C and three additional washing steps with 1× TBST (each lasting for at least 10 min), secondary antibodies coupled with horseradish peroxidase (HRP) were incubated for 45 min at room temperature. After three additional washing steps, signals were visualized using SuperSignal West Pico PLUS Chemiluminescent Substrate or SuperSignal West Femto Maximum Sensitivity Substrate (both Thermo Scientific) according to the manufacturer's protocol on the Fusion-FX6.EDGE V.070 imaging system with acquisition EVOLUTION-CAPT software (both Vilber) and further analyzed with ImageJ (Version 1.53a, Wayne Rasband, NIH) and Preview (Version 11.0, Apple). Then, membranes were stripped using Restore Western Blot Stripping Buffer (Thermo Scientific) for 20–30 min and then proceeded as described above. Antibodies used for western blotting are listed in the Supplementary Material and Methods section.

Gene expression analysis by quantitative real-time PCR

Total RNA was isolated from lysed cells and reversely transcribed using standard methods and kits according to the manufacturers' protocols (innuPREP RNA Mini Kit 2.0, IST Innuscreen; High-Capacity cDNA Reverse Transcription Kit, Applied Biosystems). The specific primer pair sequences are listed in the Supplementary Material and Methods section. Transcript amplification was visualized with the PowerUp SYBR Green Master Mix using a QuantStudio 5 Real-Time PCR System with QuantStudio Design & Analysis Software (v1.4.3) (all Applied Biosystems). The relative transcript level of each gene was calculated according to the 2−ΔΔCt method with normalization to *Actb* (β-Actin).

Bone marrow-derived dendritic cells

For co-culture with tumor cells, murine BMDCs have been generated from C57BL/6J donor-derived bone marrow cells by incubation in VLE RPMI medium supplemented with 20 ng/ml recombinant GM-CSF (Peprotech) for 8 days.

Flow cytometry

Cell suspensions were stained in phosphate-buffered saline with 1% FCS. Fluorochrome-coupled antibodies were purchased from eBioscience, BioLegend or BD Pharmingen. Anti-mouse $OVA_{257-264}$ (SIINFEKL) peptide bound to H-2Kb antibody (clone 25-D1.16) was purchased from eBioscience. iTAg MHC-I murine tetramers detecting SIINFEKL-specific $CD8^+$ T cells were purchased from MBL (Woburn, MA). Cell dyes eBioscience Fixable Viability Dye eFluor 506 and LIVE/DEAD Fixable Near-IR Dead Cell Stain Kit for 633 or 635 nm excitation (both Invitrogen) were used to assess cell viability. Data were acquired on a BD FACSCanto II Flow Cytometer (BD Biosciences) with BD FACSDiva Software (v8.0.1) and analyzed using FlowJo software 10.8.1 (TreeStar). Cell-sorting was performed on a BD FACSAria III Cell Sorter or BD FACSAria Fusion Flow Cytometer. Antibodies used for flow cytometry as well as gating strategies to define specific cell types and analyses are listed in the Supplementary Material and Methods section.

Cytokine/chemokine profiling

Conditioned culture medium harvested after 24 h from untreated or 3pRNA-treated B16 melanoma cell cultures was screened for 40 different cytokines and/or chemokines using the Proteome Profiler Mouse Cytokine Array Kit, Panel A (R&D Systems) following the manufacturer's protocol.

Tumor challenge and treatment

For the unilateral tumor model, mice were injected subcutaneously with B16.OVA (2.4×10^5) or CT26 (10^6) tumor cells. For the bilateral tumor model, mice were injected subcutaneously with B16.OVA (right flank, 2.4×10^5; left flank, 0.8×10^5) cells on day 0. Anti–CTLA-4 (clone 9H10), anti–PD-1 (clone RMP1–14), or appropriate isotype controls (200 µg; all from BioXCell, West Lebanon, NH) were administered intraperitoneally (ip) on days 6, 9 and 12 or 5, 8 and 11 for B16.OVA or CT26 tumor-bearing mice, respectively. In some B16.OVA tumor experiments, mice were additionally injected with 2 µg azacytidine (AZA) in 50 µl PBS into their flank tumor on days 6, 9 and 12. In these experiments, B16.OVA cells for tumor inoculation were harvested from *in vitro* culture during an optimal exponential growth phase to ensure aggressive *in vivo* expansion. Animals bearing bilateral tumors were injected with 25 µg 3pRNA complexed in 3.5 µl in vivo-jetPEI (Polyplus) into the right-sided tumors on days 6, 9, and 12. On some days, tumor volume was not assessed for every animal. Hence, mean tumor volume ± SEM is displayed for those assessed on that day. Mice were euthanized when the maximum tumor diameter exceeded 15 mm to 18 mm according to the standard legal procedure (responsible state office Regierung von Oberbayern). Mean tumor growth analysis was discontinued when the first animal per group succumbed to tumor progression.

Preparation of cell suspensions from tumor-draining lymph nodes

Mice were sacrificed and tumor-draining (inguinal) lymph nodes were removed using forceps and surgical scissors. Lymph nodes were minced and homogenized by sequential filtering through 100 µm and 30 µm MACS SmartStrainers (Miltenyi Biotec). Single-cell suspensions were washed in PBS before subsequent analysis.

Human tumor RNA sequencing analysis

Raw or normalized RNA sequencing counts, as well as metadata for the indicated, previously described datasets of human tumor transcriptomes were downloaded from publicly available sources as listed in the supplementary material and methods section. Transcriptomic expression data and meta information for the TCGA-SKCM data set were accessed using Bioconductor's *TCGAbiolinks* package.[22,23] In case raw counts were available for the indicated dataset, normalization was performed by the DESeq2 or edgeR workflows.[24–26] The *pyroptosis gene set* has been described previously,[27] the *RIG-I-like receptor signaling pathway gene set* was from the Kyoto encyclopedia of genes and genomes (KEGG).[28] Gene set scores were derived from transcriptomic datasets by gene-set-variation-analysis (GSVA).[29]

Statistics

If not stated otherwise, all data are presented as mean per experimental group ± standard error of the mean (SEM). Statistical analysis from cell culture experiments was based on three or more independent experiments performed in duplicate or triplicate, if not stated otherwise. The statistical significance of comparisons from cell culture experiments and *ex vivo* experiments was assessed with the independent two-tailed Student's t-test. Tumor growth data was analyzed using the open-access web tool TumGrowth.[30] Briefly, after log transformation of the data, tumor growth analysis was carried out by linear mixed-effect modeling with type II ANOVA and pairwise comparisons across groups with *p*-values being computed by the software. Overall survival was analyzed using the log-rank (Mantel-Cox) test. Normal distribution and equal standard deviation were assumed for all data. Correction for multiple testing was not performed, if not stated otherwise, as significant differences were considered to only have exploratory character. Confirmatory validation in further studies will be needed. Linear correlation between the pyroptosis and RIG-I gene set scores was investigated by Pearson correlation testing. To test for differences of the pyroptosis gene set in previously defined genomic ICI response groups,[31] the Wilcoxon-test was performed with Benjamini-Hochberg-correction for multiple testing. To compare the survival information for patients with high or low pyroptosis gene set scores, indicated cohorts were split by the median of the inferred GSVA scores. Survival estimates were generated by the Kaplan-Meier-estimator and statistical difference was tested by log-rank testing. All computation and statistical calculations for RNA-Seq analyses were performed in R version 4.3.2. Significance level was set at $p < 0.05$, $p < 0.01$, and $p < 0.001$ and was then indicated with asterisks (*, **, and ***, respectively). All statistical calculations were performed using Prism (GraphPad Software), if not stated otherwise.

Results

GSDME links active RIG-I signaling and apoptotic cell death in tumor cells to secondary pyroptosis

To assess the role of GSDME and pyroptosis in RIG-induced programmed cell death and ICI cancer immunotherapy, we used CRISPR-mediated somatic mutagenesis to generate polyclonal tumor cell lines deficient for *Gsdme* (*Gsdme*$^{-/-}$) (Figure S1). As described previously,[6] exposure of B16 murine melanoma cells to a specific RIG-I ligand (*in vitro* transcribed 5'-triphosphorylated RNA, 3pRNA) induced pro-apoptotic signaling with cleavage of the executioner caspase-3 (Figure 1a). At the same time, 3pRNA-induced selective activation of RIG-I within melanoma cells triggered cleavage of GSDME with the generation of its active N-terminal fragment, similar to exposure to the chemotherapeutic agent cisplatin. In line with that, wild-type (WT) melanoma cells undergoing RIG-I-induced

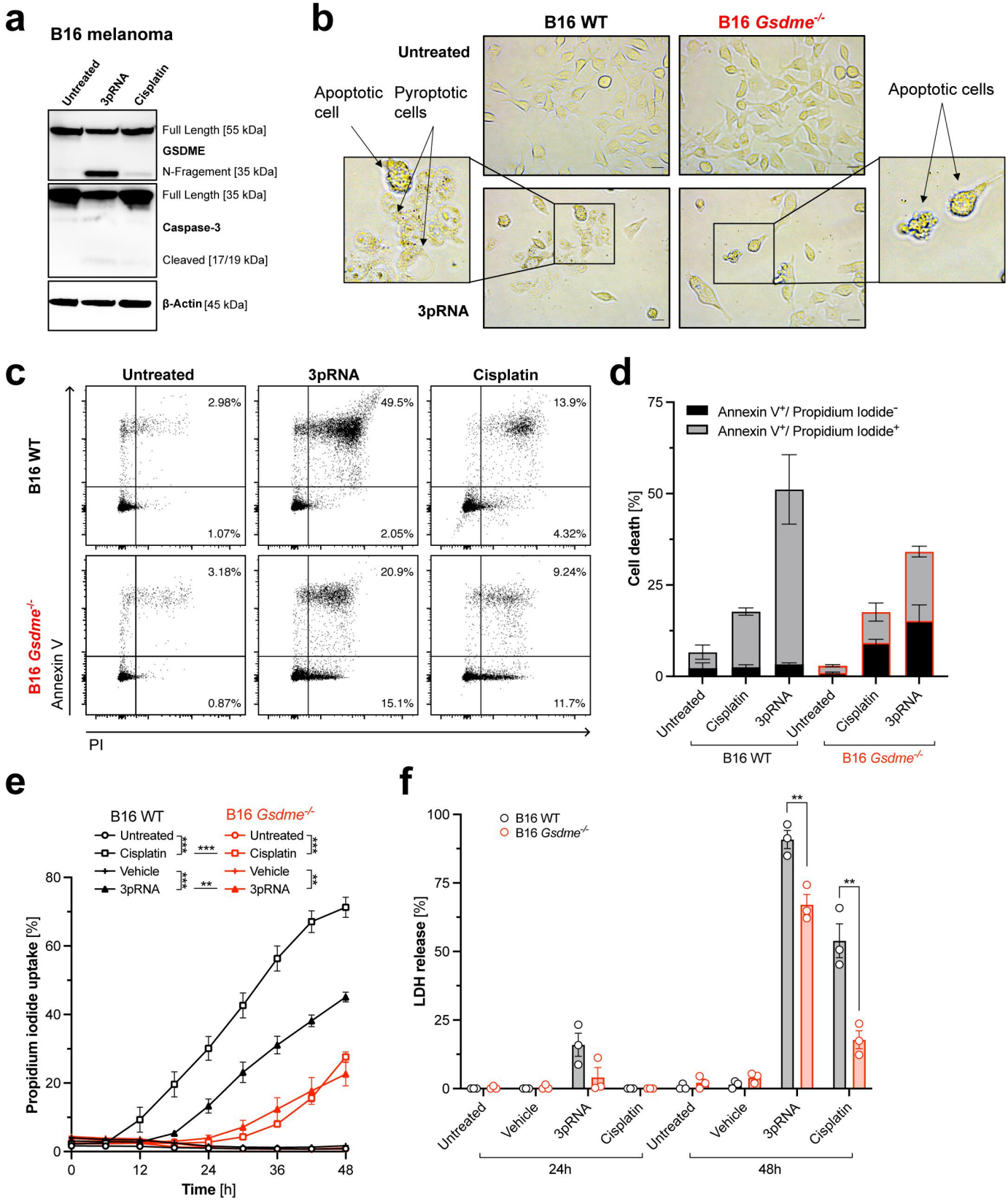

Figure 1. GSDME links active RIG-I signaling and apoptotic cell death in tumor cells to secondary pyroptosis. Wild type (WT) and *Gsdme*-deficient (*Gsdme*$^{-/-}$) B16.OVA malignant melanoma cells were exposed to the RIG-I agonist 3pRNA or the chemotherapeutic agent cisplatin. After 24 h, if not stated otherwise, the following analyses were performed. (a) Abundance of GSDME (full-length and N-terminal cleavage product) and caspase-3 (full-length and cleaved) proteins by western blot. (b) Morphological features of cell death by light microscopy; representative images with scale bar set to 20 µm. Arrows indicate ballooning of cells, typical for pyroptotic cell death, and blebbing of cells, typical for apoptosis. (c-d) Induction of regulated cell death programs was determined by Annexin V and propidium iodide (PI) staining in flow cytometry. (c) Representative dot blots and (d) bar graphs of Annexin V$^+$/PI$^-$ and Annexin V$^+$/PI$^+$ cells. (e) Uptake of PI over time by B16 cells undergoing regulated cell death was continuously determined by live-cell analysis. (f) Leakage of LDH as a surrogate marker of loss of cell membrane integrity measured in B16 cell culture supernatant (normalized to total cellular LDH content) at the indicated time points. All graphs show mean data ± SEM of at least triplicate samples that are either pooled from or representative of at least two independent experiments. WT, wild type.

regulated cell death showed morphological features of both apoptosis (with membrane blebbing and fragmentation) as well as (secondary) pyroptosis (with ballooning as a sign of plasma cell permeabilization and subsequent cell swelling) (Figure 1b). In contrast, RIG-I activation in *Gsdme*$^{-/-}$ melanoma cells morphologically almost exclusively resulted in apoptotic but rarely in pyroptotic cell death.

Active RIG-I signaling or exposure to cisplatin resulted in pro-apoptotic signaling in tumor cells with binding of annexin V, a surrogate marker of structural changes in the plasma cell membrane during apoptosis (Figure 1c,d). In line with the pore-forming function of GSDME activated by 3pRNA or cisplatin, apoptosis was followed by secondary loss of cell membrane integrity with uptake of the DNA-intercalating dye propidium iodide (PI), which is typically excluded from cells with plasma membrane integrity. In *Gsdme*$^{-/-}$ tumor cells, the overall extent of RIG-I-induced programmed cell death trended to be reduced, while the fraction of cells undergoing secondary pyroptosis with cell membrane permeabilization was significantly diminished (*, $p = 0.039$). Loss of plasma cell membrane integrity during RIG-I-induced cell death became apparent after 18–24 hours and was both delayed and reduced in its extent in *Gsdme*$^{-/-}$ melanoma cells (Figure 1e). Loss of cell membrane integrity was also associated with leakage of cytosolic components, such as the enzyme L-lactatdehydrogenase (LDH), which was less pronounced in *Gsdme*$^{-/-}$ tumor cells (Figure 1f). RIG-induced cleavage of GSDME associated with secondary pyroptotic cell death was similarly observed in YUMMER1.7 melanoma cells with a distinct genetic background as well as CT26 colon adenocarcinoma cells derived from a different mouse strain (Figure S2). Taken together, these data suggest that active RIG-I signaling in tumor cells leads to the cleavage and activation of GSDME, which can transition apoptotic cell death to secondary pyroptosis with loss of cell membrane integrity and release of cytosolic components.

Defective GSDME renders tumors resistant to ICI immunotherapy

To address the role of GSDME and (secondary) pyroptosis for the efficacy of ICI immunotherapy, mice were subcutaneously inoculated with either WT or *Gsdme*$^{-/-}$ B16 melanoma cells expressing the model antigen ovalbumin (OVA) (Figure 2a). Upon treatment with anti-CTLA-4 immunotherapy, ICI-induced tumor control was indeed largely abrogated in mice bearing *Gsdme*$^{-/-}$ melanomas, which was associated with poor overall host survival (Figure 2b,c). Also, for the clinically more relevant combination of anti-PD-1 and anti-CTLA-4, we found reduced anti-tumor activity in mice bearing melanoma with genetic deficiency for GSDME (Figure 2d). In this, *Gsdme*$^{-/-}$ tumors phenocopied the poor susceptibility to ICI immunotherapy that we have previously described for RIG-I-deficient tumors.[6] In contrast to a recent study in murine EMT6 mammary and CT26 colon carcinomas,[32] in the absence of ICI immunotherapy, we did not observe more aggressive tumor growth of *Gsdme*$^{-/-}$ B16 melanomas when comparing to their WT counterparts (Figure 2b), suggesting that GSDME-independent effects can additionally limit immunosurveillance in untreated B16 melanomas. Similarly, in mice bearing CT26 colonic adenocarcinoma tumors, we observed a trend for reduced anti-tumor activity of anti-CLTA-4 treatment with *Gsdme*$^{-/-}$ tumors (Figure S3a-b).

We and others have previously shown that targeted activation of the RIG-I pathway in tumor cells is a viable therapeutic strategy to trigger immunogenic tumor cell death that can foster the induction of systemic antitumor T-cell immunity and render tumors susceptible to ICI immunotherapy.[6,33,34] In line with the above-described importance of tumor cell-intrinsic GSDME to link RIG-I-mediated pro-apoptotic signaling to inflammatory pyroptotic tumor cell death, we found that the antitumor activity of ligand-induced RIG-I signaling in the TME and its combination with ICI relied on GSDME activity in tumor cells (Figure S3c-f). Of note, our data suggest that the synergistic effects of targeting RIG-I in the TME and ICI have a component that is independent of tumor-intrinsic *Gsdme*, presumably mediated by RIG-I activation in innate immune cells and associated pro-inflammatory cytokine release.[6] Taken together, our data demonstrate that ICI immunotherapy in murine melanoma relies on GSDME-mediated tumor cell pyroptosis, which can be enhanced by therapeutic targeting of the RIG-I pathway within tumor cells.

Antigen cross-presentation by cDC1s and subsequent ICI-enhanced expansion of reactive cytotoxic T cells relies on tumor cell-intrinsic GSDME activity

Next, we assessed whether defects in GSDME-mediated pyroptosis in tumor cells impacted DC functionality and the formation of ICI-enhanced anti-tumor T-cell responses, using our established model of *Gsdme*$^{-/-}$ B16 melanoma-bearing mice (Figure 3a). The subtype of conventional type 1 DCs (cDC1s) has been associated with beneficial survival in cancer patients and was found critical for the spontaneous rejection of immunogenic cancers and the success of T cell-based immunotherapies in preclinical murine models.[35] The unique role of cDC1s is reflected in part by their ability to initiate *de novo* T-cell responses after migrating to tumor-draining lymph nodes, as well as to cross-present tumor antigens within the TME, enhancing local cytotoxic T-cell function. In adjacent tumor-draining lymph nodes of *Gsdme*$^{-/-}$ melanomas, we found poor activation of cDC1s compared to wild-type tumors with reduced expression of the co-stimulatory molecule CD86 (Figure 3b). Similarly, processing of the tumor-associated antigen OVA and cross-presentation of its immune-dominant peptide epitope SIINFEKL by MHC-I on cDC1s in draining lymph nodes of *Gsdme*$^{-/-}$ tumors was reduced compared to mice bearing wild-type tumors (Figure 3c).

Reduced cross-presentation associated with *Gsdme*$^{-/-}$ tumors resulted in impaired ICI-mediated cross-priming and expansion of tumor antigen-specific cytotoxic T cells. The anti-CTLA-4 immunotherapy effect with potently enhanced numbers of circulating tumor model antigen OVA-specific CD8^{+} T cells in mice bearing wild-type melanomas was largely abrogated in mice with *Gsdme*$^{-/-}$ tumors (Figure 3d,e). In contrast to EMT6 murine mammary carcinomas,[32] defects in T-cell expansion with *Gsdme*$^{-/-}$ B16 melanomas became evident only during ICI immunotherapy, suggesting GSDME-independent T-cell

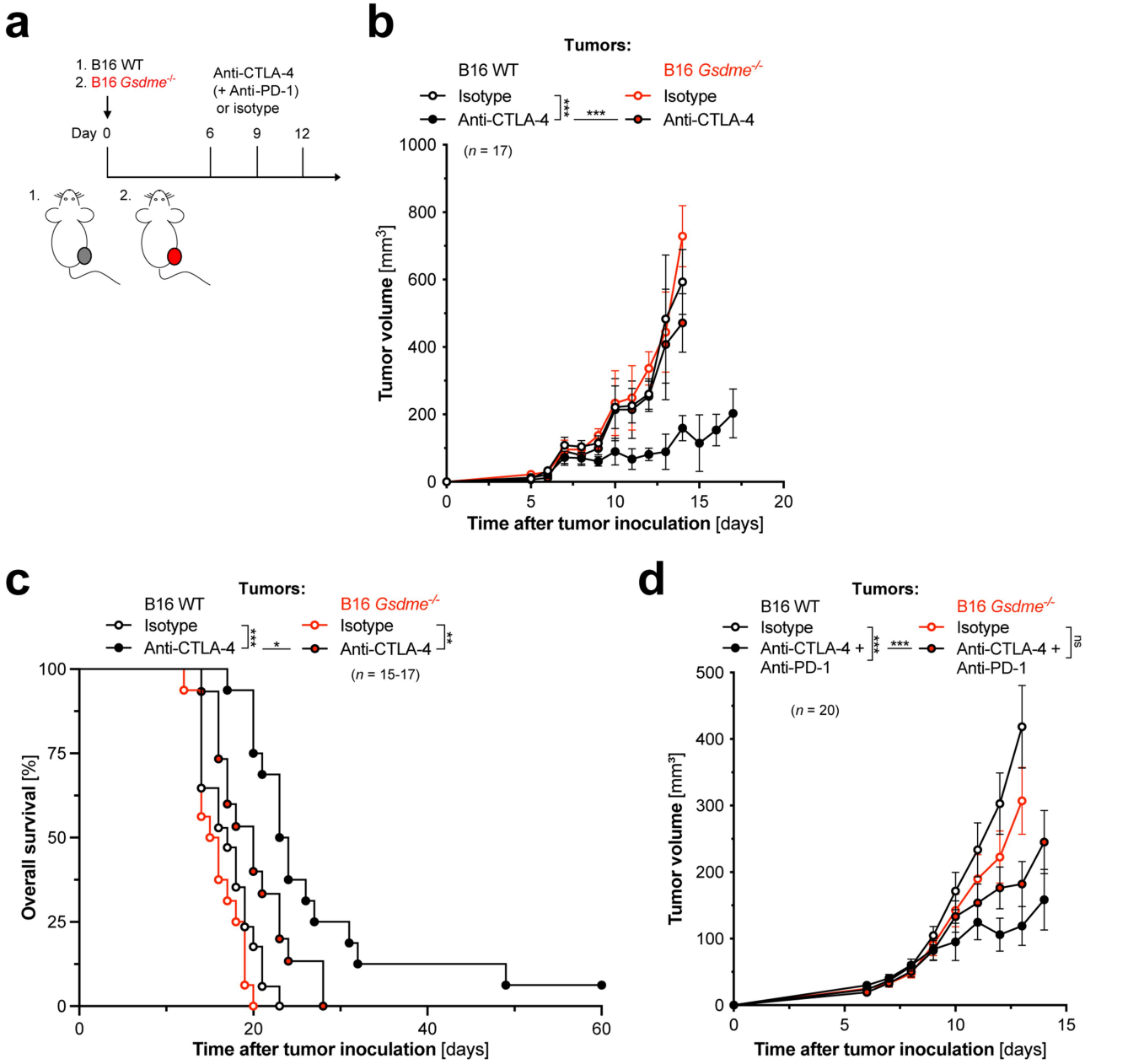

Figure 2. Defective GSDME renders tumors resistant to ICI immunotherapy. (a) Treatment scheme: C57BL6/J mice were inoculated with either WT or *Gsdme*$^{-/-}$ B16.OVA malignant melanoma cells. Tumor-bearing mice were treated with anti-CTLA-4 ± anti-PD-1 or isotype control antibodies on days 6, 9 and 12. (b) Tumor growth and (c) overall survival in mice after anti-CTLA-4 ICI immunotherapy. (d) Tumor growth in mice after anti-CTLA-4 + anti-PD-1 combinatorial ICI immunotherapy. All data show mean tumor volume ± SEM or survival of $n = 15–20$ individual mice per group that were pooled from at least three independent experiments.

immunosuppressive factors associated with B16 melanomas. Moreover, we co-cultured bone marrow-derived dendritic cells (BMDCs) with fluorescently (CFSE)-labeled B16 tumor cells undergoing RIG-I- or Cisplatin-induced programmed cell death. We then measured the frequency of CFSE^{+} BMDCs as a correlate for uptake of tumor cell debris. Deficiency for *Gsdme* in dying tumor cells resulted in reduced uptake by bystander BMDCs (Figure 3f). To identify factors that may contribute to the immunogenicity of RIG-I/GSDME-driven pyroptotic tumor cell death, we performed a broad cytokine/chemokine screen from the culture supernatant of both WT and *Gsdme*$^{-/-}$ B16 melanoma cells undergoing RIG-I-induced programmed cell death (Figure 3g). Among the factors for which release was most prominently impaired in *Gsdme*$^{-/-}$ tumor cells were the pro-inflammatory cytokines IL-6 and TNF-α as well as the chemokine CXCL9. Taken together, these data show that defective GSDME in tumor cells reduced release of pro-inflammatory factors from dying cells associated with impaired tumor cell uptake and tumor antigen cross-presentation by cDC1s, resulting in suboptimal expansion of tumor antigen-specific T cells and, ultimately, poor tumor control upon ICI immunotherapy.

Epigenetic reprogramming with upregulation of GSDME enhances melanoma susceptibility to RIG-I-induced cell death

First identified in breast cancer patients, epigenetic silencing of *GSDME* seems to be a common pattern to evade

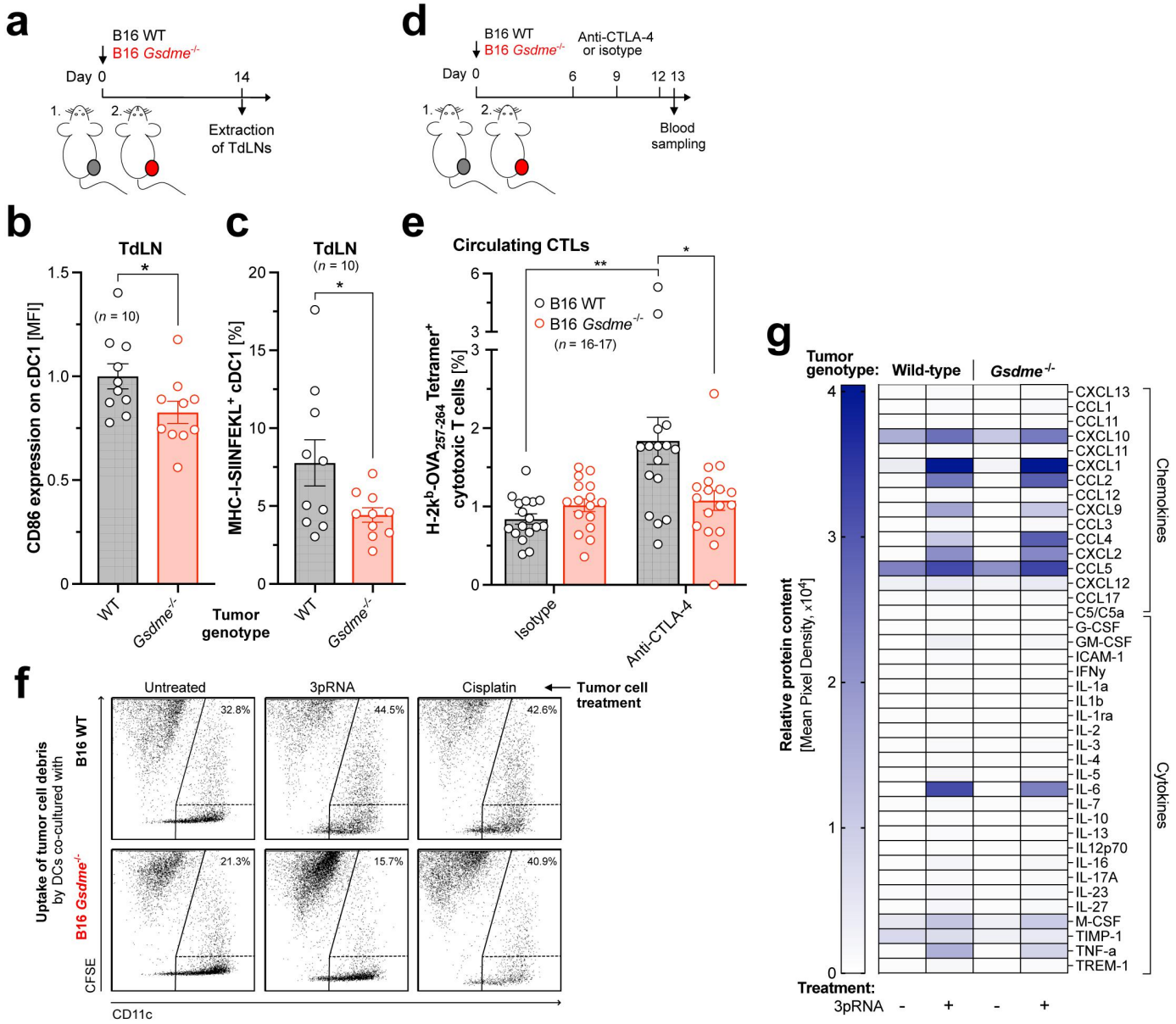

Figure 3. Antigen cross-presentation by cDc1s and subsequent ICI-enhanced expansion of reactive cytotoxic T cells relies on tumor cell-intrinsic GSDME activity. (a) Experimental setup 1: C57Bl6/J mice were inoculated with either WT or *Gsdme*$^{-/-}$ B16.OVA tumor cells. Tumor-draining lymph nodes (TdLNs) were extracted on day 14 and analyzed by flow cytometry. (b) Expression of CD86 (c) as well as cross-presentation of the processed OVA peptide-epitope SIINFEKL in the context of MHC-I on conventional type 1 dendritic cells (cDC1) cells in TdLNs. CD86 expression was normalized to cDc1s from WT B16.OVA-bearing mice. (d) Experimental setup 2: C57Bl6/J mice were inoculated with either WT or *Gsdme*$^{-/-}$ B16.OVA tumor cells. Mice were treated with anti-CTLA-4 or isotype control antibodies on days 6, 9 and 12 as described for Figure 2. Blood was sampled on day 13 and analyzed by flow cytometry. (e) Frequency of circulating H-2k^{b}-SIINFEKL Tetramer^{+} CD8^{+} T cells in the peripheral blood. All data give mean values ± SEM of $n = 10–17$ individual mice per group that were pooled from at least two independent experiments (f) B16 melanoma cells were labeled with CFSE prior to *in vitro* exposure to 3pRNA or cisplatin for 24 hours. Bone marrow-derived dendritic cells (BMDCs) were subsequently short-time (4 h) co-cultured with B16 cells undergoing programmed cell death, and uptake of fluorescently labeled tumor cell debris by BMDCs was analyzed via flow cytometry. Representative dot blots give the percentage of CD11c^{+} BMDCs with positive co-staining for CFSE. (g) Heatmap showing the relative release of cytokines and chemokines from WT or *Gsdme*$^{-/-}$ B16.OVA cells in response to RIG-I activation *in vitro*. TdLN, tumor-draining lymph node; cDC1, conventional type 1 dendritic cell; BMDC, bone marrow-derived dendritic cell.

immunosurveillance in a variety of human cancers.[17,18] A meta-analysis has found hypermethylation in the promoter region of *GSDME* associated with reduced transcriptional activity to be much more frequent in human cancer samples in comparison to healthy tissue controls.[36] As described previously,[16] hypomethylating agents such as 5-azacytidine (AZA) can revert epigenetic silencing and induce expression of *Gsdme* in cancer cells (Figure 4a and S4a). Tumor cell exposure to AZA did not enhance the transcriptional activity of components of the RIG-I pathway, caspase-3 (*Casp3*) or IFN-β (*Ifnb1*) (Figure S4b). Low-dose AZA treatment without direct cytotoxic effects potently enhanced B16 melanoma cell susceptibility to RIG-I-mediated inflammatory cell death with loss of tumor cell plasma membrane integrity and subsequent leakage of cytosolic components (Figure 4b,c and S4c). Such AZA-induced epigenetic reprogramming of melanoma cells to favor the transition to pyroptotic cell death upon RIG-I activation was completely dependent on GSDME activity. In mice

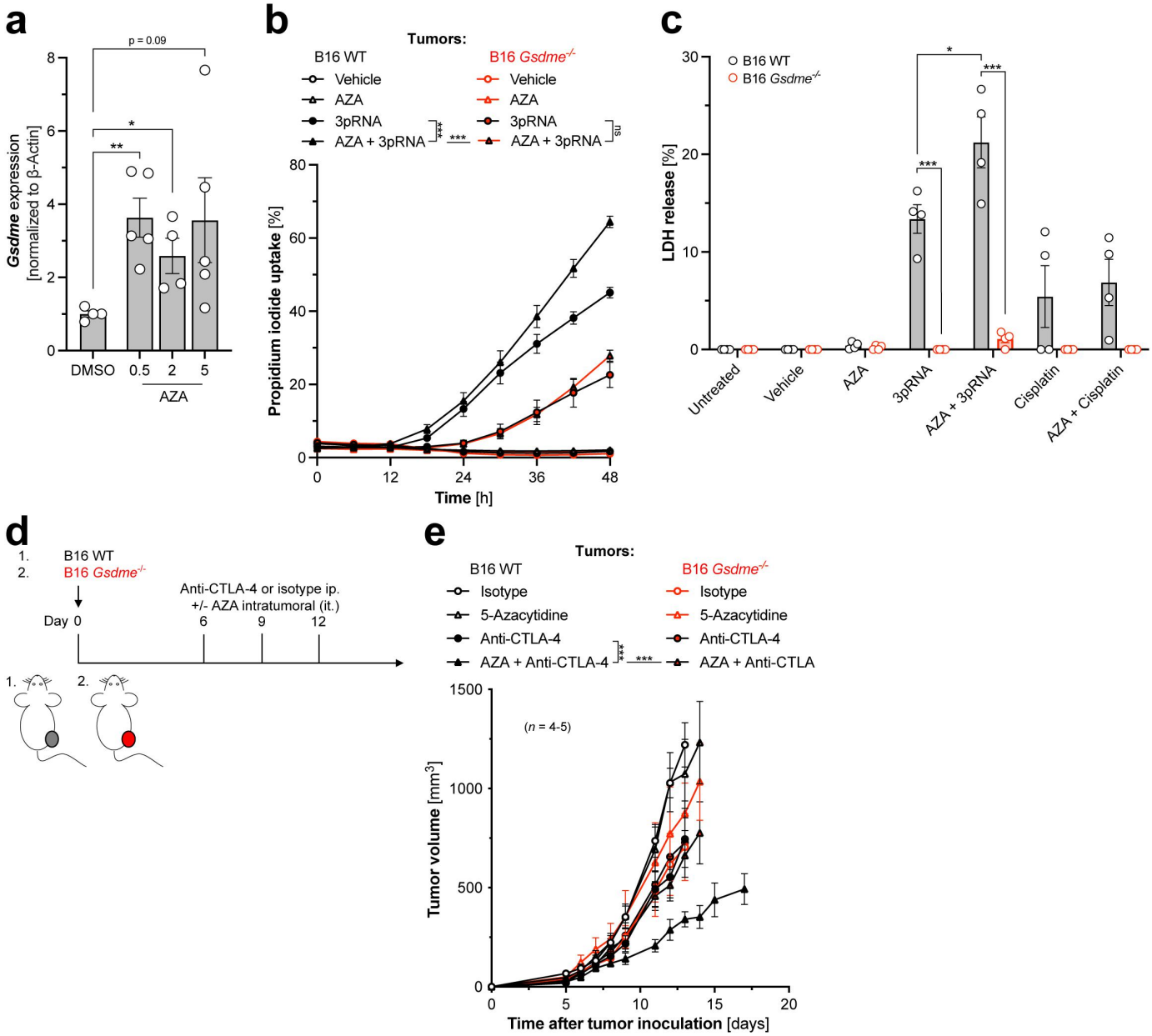

Figure 4. Epigenetic reprogramming with upregulation of *Gsdme* enhances melanoma susceptibility to ICI immunotherapy. (a) B16.OVA cells were exposed to 5-azacytidine (AZA) for 96 hours. Expression of GSDME was determined by western blot and quantitative analysis was normalized to ß-actin. (b-c) WT and *Gsdme*$^{-/-}$ B16.OVA cells were exposed to AZA for 48 hours before they were treated with 3pRNA or cisplatin. (b) Uptake of PI over time by B16.OVA cells undergoing regulated cell death was continuously determined by live-cell analysis. (c) Leakage of LDH was measured in the B16.OVA cell culture supernatant (normalized to total cellular LDH content) at the indicated time points. Data give mean values ± SEM pooled from at least three independent experiments. (d) Treatment scheme: WT mice were inoculated with either WT or *Gsdme*$^{-/-}$ B16.OVA cells. Recipients were injected intraperitoneally with anti-CTLA-4 or isotype control antibodies in combination with intratumoral application of AZA. (e) Mean tumor volume ± SEM of $n = 4$-5 individual mice per group. Data are representative of two independent experiments. ip, intraperitoneal; it, intratumoral.

bearing wild-type melanoma, intratumoral injection of low-dose AZA combined with systemic ICI immunotherapy synergistically improved tumor control (Figure 4d,e). In contrast, in mice bearing tumors with irreversible genetic *Gsdme* deficiency, epigenetic combination therapy with AZA failed to render tumors susceptible to ICI treatment. In summary, these findings suggest that combination therapy with hypomethylating agents (e.g. AZA) has the potential to overcome tumor resistance to ICI immunotherapy by upregulation of otherwise epigenetically silenced components of the pyroptosis cell death pathway in tumor cells.

High transcriptional activity of a pyroptosis gene set correlates with RIG-I pathway activity and is associated with beneficial response to ICI therapy in melanoma patients

To assess the clinical relevance of our findings, we analyzed the transcriptional activity of a pre-defined set of 14 pyroptosis-associated genes[27] (including *GSDME*, Figure S5a) in 463 primary melanoma patient samples from The Cancer Genome Atlas (TCGA)[37] determined by RNA-Seq. We have previously shown that high expression of *RIG-I* in human melanoma is associated with prolonged survival and durable responses to

ICI immunotherapy.[6] We now found that transcriptional activity of the *pyroptosis gene set*, but not *GSDME* as a single gene, correlated strongly with the expression of a *RIG-I pathway gene set* in human melanoma (Figures 5a and S5b-c). In retrospective analysis, high tumor expression of the *pyroptosis gene set* was associated with prolonged overall survival in malignant melanoma patients (Figure 5b).

Next, we retrospectively analyzed pre-treatment tumor RNA-Seq data from three previously described cohorts of malignant melanoma patients undergoing anti-PD-1 and/or anti-CTLA-4 immunotherapy. In line with our preclinical data, low transcriptional activity of the *pyroptosis gene set* in tumors was associated with cancer resistance and disease progression in malignant melanoma patients undergoing combined anti-PD-1/anti-CTLA-4 immunotherapy (Figure 5c).[38] In two separate melanoma patient cohorts,[39,40] high expression of the *pyroptosis gene set* in tumors tended to be associated with prolonged progression-free and overall survival following immunotherapy with anti-PD-1 ± anti-CTLA-4 (Figure S5d-e). However, they did not meet levels of statistical significance, presumably due to the small cohort size. Taken together, these patient data corroborate our preclinical findings that high activity of GSDME-based pyroptosis in melanoma tissue is associated with prolonged overall survival and favorable responses to ICI immunotherapy.

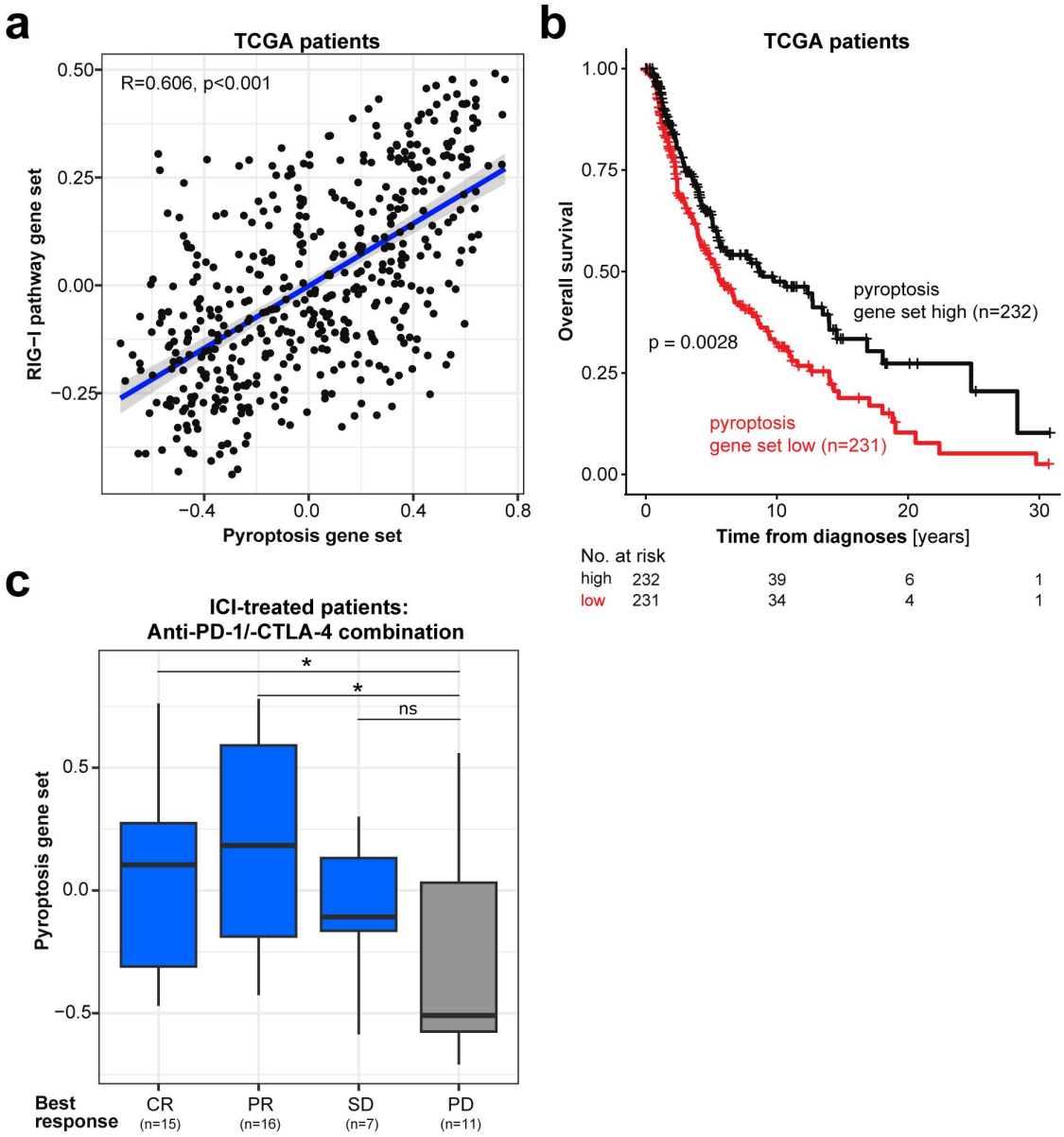

Figure 5. High transcriptional activity of a pyroptosis gene set correlates with RIG-I pathway activity and is associated with beneficial response to ICI therapy in melanoma patients. (a) Scatter plot comparing GSVA signature scores of a pyroptosis versus a RIG-I pathway gene set using RNA-seq data from TCGA cutaneous melanoma patient samples. Pearson correlation coefficient (R) and *p* values are displayed. (b) Overall survival in 463 patients with malignant melanoma from TCGA stratified by pyroptosis GSVA signature scores in tumor samples. (c) Comparison of pre-treatment *pyroptosis* gene set GSVA signature scores in 49 malignant melanoma patients stratified by individual best response to combined anti-PD-1/anti-CTLA-4 ICI immunotherapy. CR, complete response; PD, progressive disease; PR, partial response; SD, stable disease.

Discussion

The here proposed concept that ICI immunotherapy depends on tumor cell-intrinsic GSDME activity is in line with previous reports demonstrating that artificial activation of the GSDME pyroptosis pathway can boost ICI immunotherapy. Oncolytic herpes simplex virus has been used to upregulate GSDME expression levels through reduced ubiquitination and degradation, and together with a DNA methyltransferase inhibitor nanoprodrug remodeled the immunosuppressive TME and improved the efficacy of ICI therapy.[41] A recombinant adeno-associated virus expressing the N-terminal gasdermin domain was able to induce pyroptosis and prolong survival in preclinical cancer models, which was further improved in combination with anti-PD-L1.[42] Tigilanol tiglate, a protein kinase C/C1 domain activator currently undergoing early-phase clinical testing, has been found to directly activate caspase/GSDME-dependent pyroptotic signaling in tumors, hence rendering B16-F10 murine melanomas susceptible to ICI immunotherapy.[43] While these studies provided important mechanistic learnings, they are based on highly artificial modes of pyroptosis induction. In contrast, our approach with tumor-intrinsic genetic deletion of *Gsdme* suggests some level of spontaneous and potentially continuous pro-pyroptotic signaling in tumor cells as an ignition point of basal T-cell immunity and a prerequisite for the success of subsequent ICI immunotherapy. This aligns with a previous report in which loss of *Gsdme* in certain murine tumors was associated with reduced infiltration of activated T cells and overall poor tumor immunosurveillance.[21]

Even though GSDME is one of the most widely expressed members of the gasdermin family and is evolutionary highly conserved,[11] suggesting an important role in cell homeostasis, possible redundant functions with other gasdermins in cancer are emerging. In humans, the family of gasdermins has six members (GSDMA, GSDMB, GSDMC, GSDMD, GSDME and PJVK), all of which – except PJVK – carry an N-terminal domain that harbors intrinsic pore-forming and pyroptosis-inducing capacity.[11] Triggering pyroptosis in less than 15% of tumor cells via tumor-selective release of GSDMA3 with a bioorthogonal chemical system was found sufficient to induce elimination of the entire mammary tumor graft in mice.[44] Enforced expression of human GSDMB in cancer cells has been used to enhance tumor clearance in a mouse model.[45] Non-canonical nuclear PD-L1 expression has been suggested to switch TNF-α-induced apoptosis to pyroptosis in cancer cells via caspase-8-mediated cleavage of GSDMC.[46] These data suggest that multiple GSDMs can facilitate immunogenic pyroptotic tumor cell death. The different roles of particular GSDM family members are likely dependent on their degree of expression in the tumor tissue, and high variability in tissue-specific expression of different GSDMs has been described.[11] However, the role of GSDMs other than GSDME for the treatment efficacy of immunotherapies, including ICI, remains unclear.

The exact mechanisms that may perpetuate the here proposed basal pro-pyroptotic signaling in tumors remain to be determined. Several reports suggested that the cytotoxic activity of tumor-infiltrating immune cells can trigger pyroptosis in cancer cells. Granzyme B released from cytotoxic T cells and NK cells was found to directly cleave GSDME, which resulted in pyroptotic cell death.[32] Quite similarly, granzyme A has been shown to cleave and activate GSDMB.[45] We here propose that tumor cell-intrinsic innate immune signaling via the RNA receptor RIG-I triggers basal apoptosis induction and subsequent GSDME-mediated transition to pyroptosis. Indeed, genetically engineered tumors deficient in nucleic acid receptor systems including RIG-I/MAVS phenocopied tumor resistance to ICI with *Gsdme*$^{-/-}$ tumors.[6,47] Interestingly, previous studies in the context of viral infection have also linked RIG-I signaling to pyroptosis. Programmed cell death induced by infection with vesicular stomatitis virus, whose RNA is readily detected by RIG-I, has been shown to trigger proinflammatory cleavage of GSDME.[15] Similarly, recognition of Zika virus genomic RNA by RIG-I, followed by activation of caspase-3 can ultimately result in GSDME-mediated pyroptotic cell death of host immune cells.[48] Aberrantly located self RNA and DNA leaked from the nucleus, particularly under genotoxic stress conditions, have been suggested as potential endogenous ligands for nucleic acid receptor signaling in cancer cells. While our data provide a rationale for the importance of the RIG-I/MAVS/Caspase-3/GSDME axis *in vivo* to facilitate ICI-mediated antitumor immunity, alternative and possibly redundant upstream pathways might similarly trigger cleavage of GSDME. It is important to mention that progression to lytic and inflammatory pyroptosis via GSDME is a broad reaction pattern in apoptotic (tumor) cells in case they are not scavenged by APCs. A multitude of stimuli that commonly result in cleavage of the executioner caspase-3 and associated apoptotic tumor cell death principally have the potential to trigger secondary pyroptosis in case of insufficient efferocytosis in the TME.

Regarding tumor cell-derived factors that drive immunogenicity of programmed cell death via the RIG-I/caspase-3/GSDME axis, we and others have previously demonstrated that RIG-I-induced immunogenic cell death occurs independent of the interaction of ATP with the purinergic receptor P2X7 or NLRP3 as well as HMGB1 detection by TLR4 or RAGE.[6,8] Therefore, a critical (i.e. non-redundant) role of the constitutive DAMPs ATP or HMGB1 in this context seems highly unlikely. Here, we show that tumor cell-intrinsic defects in GSDME were associated with impaired release of the pro-inflammatory cytokines IL-6 and TNF-α as well as the chemokine CXCL9 from tumor cells undergoing RIG-I-induced cell death. IL-6 and TNF-α have been associated with immunogenic cell death in the past.[49] CXCL9 produced by intratumoral cDC1s has previously been found critical for antitumor T-cell responses and ICI immunotherapy.[50] Taken together, these data suggest that tumor cell-released inducible (rather than constitutive) DAMPs, including pro-inflammatory cytokines and chemokines, may contribute to the immunogenicity of RIG-I/caspse-3/GSDME-driven pyroptotic tumor cell death.

Other forms of immunogenic cell death have been linked to tumor immunosurveillance and the efficacy of ICI. Necroptosis is executed once RIPK3 phosphorylates and oligomerizes the pore-forming protein MLKL. Forced overexpression of *Mlkl*-encoding mRNA in CT26 colon carcinoma or B16 melanoma resulted in IFN-I-dependent cross-priming of CD8$^+$ T cells by migratory DCs and subsequent tumor eradication upon ICI

treatment.[51] Injection of genetically engineered tumor cells expressing a constitutively active form of RIPK3 synergized with ICI immunotherapy for durable tumor clearance in mice.[52] Growing evidence of plasticity in programmed cell death pathways has led to the development of the concept of PANoptosis, an inflammatory cell death process that combines elements from necroptosis, apoptosis, and pyroptosis.[53] PANoptosis cannot be fully explained by any single canonical cell death pathway and is thought to play a role in innate immune responses, potentially influencing tumor immunosurveillance as well.[54] Analysis of the human cancer transcriptome has indicated tumor-type-specific variations in the activity of regulated cell death pathways.[53] The field is generally challenged by a lack of reliable markers to distinguish apoptosis from different forms of regulated inflammatory cell death *in-vivo*.[12] Currently, it is still unclear to what extent redundancy exists among different cell death pathways, and how these mechanisms individually impact tumor immunosurveillance in a context-dependent manner.

In this study, we have demonstrated that basal GSDME activity and associated pyroptotic tumor cell death are necessary for the efficacy of ICI in cancer. A better understanding of the complex and potentially redundant function of other gasdermins, and the demarcation from other forms of regulated cell death in cancer will be needed for therapeutic exploitation of the pyroptosis pathway to the benefit of cancer patients. It could offer support to explore new combinatorial therapeutic regimes, including specific RIG-I agonists to enhance tumor cell-intrinsic GSDME activity and subsequent immunogenic pyroptosis to overcome cancer resistance to established ICI immunotherapies, particularly in immunologically "cold" tumors.

Acknowledgments

This work is part of the doctoral thesis of S.E. and A.S. at the Technical University of Munich. We thank Emad S. Alnemri (Thomas Jefferson University, Philadelphia, PA) for providing a *Gsdme*$^{-/-}$ B16 cell line that was used for initial preliminary experiments. We thank Tatiana Nedelko (Munich) and Maria Krieger (Regensburg) for excellent technical support.

Disclosure statement

S.H. is a consultant for Bristol Myers-Squibb, Novartis, Merck, Abbvie, and Roche. S.H. has received research funding from Bristol Myers-Squibb and Novartis. S.H. is an employee of and holds equity interest in Roche/Genentech. M.P. received travel grants and honoraria from Kite and Takeda. H.P. is a consultant for Gilead, Abbvie, Pfizer, Novartis, Servier, and Bristol Myers-Squibb. H.P. has received research funding from Bristol Myers-Squibb. The remaining authors declare no financial conflict of interest.

Funding

This study was supported by Wilhelm Sander Foundation (2021.041.1 to S.H., 2021.040.1 to H.P., 2023.101.1 to N.E.K.), Melanoma Research Alliance (Young Investigator Award to S.H.), the German José Carreras Foundation (DJCLS 07 R/2020 to S.H), European Hematology Association (to N.E.K.), Deutsche Forschungsgemeinschaft (DFG, German Research Foundation) – project number 360372040 – SFB 1335 (to H.P. and F.B.), project number 395357507 – SFB 1371 (to H.P), project number 324392634 – TRR 221 (to H.P), TRR 387/1 – 514894665 and DFG BA 2851/6-1 (project ID: 452409123) and DFG BA 2851/7-1 (project ID: 537477296) to F.B., Bavarian Cancer Research Centre (BZFK; to H.P.) and the German Cancer Aid (70114547 to H.P.).

ORCID

Simon Heidegger http://orcid.org/0000-0001-6394-5130

Author contributions

S.E. and S.H. designed the research, analyzed and interpreted the results. S.E., A.S., and N.E.K. performed experiments. S.E. and J.C.E. analyzed human cancer transcriptome data sets. S.E. and S.H. prepared the manuscript. N.S., P.M., M.P., K.K., J.R., F.B., and H.P. gave methodological support and conceptual advice. S.H. guided the study.

Availability of data and material

This study did not generate novel code or big data sets. Primary data will be shared upon reasonable request with the corresponding author.

References

1. Morad G, Helmink BA, Sharma P, Wargo JA. Hallmarks of response, resistance, and toxicity to immune checkpoint blockade. Cell. 2021;184(21):5309–5337. doi: 10.1016/j.cell.2021.09.020.
2. Wolchok JD, Chiarion-Sileni V, Gonzalez R, Grob JJ, Rutkowski P, Lao CD, Cowey CL, Schadendorf D, Wagstaff J, Dummer R, et al. Long-Term outcomes with Nivolumab plus Ipilimumab or Nivolumab alone versus Ipilimumab in patients with advanced melanoma. J Clin Oncol. 2022;40(2):127–137. doi: 10.1200/JCO.21.02229.
3. Robert C. A decade of immune-checkpoint inhibitors in cancer therapy. Nat Commun. 2020;11(1):3801. doi: 10.1038/s41467-020-17670-y.
4. Havel JJ, Chowell D, Chan TA. The evolving landscape of biomarkers for checkpoint inhibitor immunotherapy. Nat Rev Cancer. 2019;19(3):133–150. doi: 10.1038/s41568-019-0116-x.
5. Zitvogel L, Galluzzi L, Kepp O, Smyth MJ, Kroemer G. Type I interferons in anticancer immunity. Nat Rev Immunol. 2015;15(7):405–414. doi: 10.1038/nri3845.
6. Heidegger S, Wintges A, Stritzke F, Bek S, Steiger K, Koenig PA, Göttert S, Engleitner T, Öllinger R, Nedelko T, et al. RIG-I activation is critical for responsiveness to checkpoint blockade. Sci Immunol. 2019;4(39):4. doi: 10.1126/sciimmunol.aau8943.
7. Besch R, Poeck H, Hohenauer T, Senft D, Häcker G, Berking C, Hornung V, Endres S, Ruzicka T, Rothenfusser S, et al. Proapoptotic signaling induced by RIG-I and MDA-5 results in type I interferon–independent apoptosis in human melanoma cells. J Clin Invest. 2009;119:2399–2411. doi: 10.1172/JCI37155.
8. Duewell P, Steger A, Lohr H, Bourhis H, Hoelz H, Kirchleitner SV, Stieg MR, Grassmann S, Kobold S, Siveke JT, et al. RIG-I-like helicases induce immunogenic cell death of pancreatic cancer cells and sensitize tumors toward killing by CD8(+) T cells. Cell Death Differ. 2014;21(12):1825–1837. doi: 10.1038/cdd.2014.96.
9. Poeck H, Besch R, Maihoefer C, Renn M, Tormo D, Morskaya SS, Kirschnek S, Gaffal E, Landsberg J, Hellmuth J, et al. 5′-triphosphate-siRNA: turning gene silencing and rig-I activation against melanoma. Nat Med. 2008;14(11):1256–1263. doi: 10.1038/nm.1887.
10. Tsuchiya K. Switching from apoptosis to Pyroptosis: gasdermin-elicited inflammation and antitumor immunity. Int J Mol Sci. 2021;22(1):22. doi: 10.3390/ijms22010426.
11. Broz P, Pelegrín P, Shao F. The gasdermins, a protein family executing cell death and inflammation. Nat Rev Immunol. 2020;20(3):143–157. doi: 10.1038/s41577-019-0228-2.

12. Meier P, Legrand AJ, Adam D, Silke J. Immunogenic cell death in cancer: targeting necroptosis to induce antitumour immunity. Nat Rev Cancer. 2024;24(5):299–315. doi: 10.1038/s41568-024-00674-x.
13. Galluzzi L, Buqué A, Kepp O, Zitvogel L, Kroemer G. Immunogenic cell death in cancer and infectious disease. Nat Rev Immunol. 2017;17(2):97–111. doi: 10.1038/nri.2016.107.
14. Wang Y, Gao W, Shi X, Ding J, Liu W, He H, Wang K, Shao F. Chemotherapy drugs induce pyroptosis through caspase-3 cleavage of a gasdermin. Nature. 2017;547(7661):99–103. doi: 10.1038/nature22393.
15. Rogers C, Fernandes-Alnemri T, Mayes L, Alnemri D, Cingolani G, Alnemri ES. Cleavage of DFNA5 by caspase-3 during apoptosis mediates progression to secondary necrotic/pyroptotic cell death. Nat Commun. 2017;8(1):14128–. doi: 10.1038/ncomms14128.
16. Akino K, Toyota M, Suzuki H, Imai T, Maruyama R, Kusano M, Nishikawa N, Watanabe Y, Sasaki Y, Abe T, et al. Identification of DFNA5 as a target of epigenetic inactivation in gastric cancer. Cancer Sci. 2007;98(1):88–95. doi: 10.1111/j.1349-7006.2006.00351.x.
17. Fujikane T, Nishikawa N, Toyota M, Suzuki H, Nojima M, Maruyama R, Ashida M, Ohe-Toyota M, Kai M, Nishidate T, et al. Genomic screening for genes upregulated by demethylation revealed novel targets of epigenetic silencing in breast cancer. Breast Cancer Res Treat. 2010;122(3):699–710. doi: 10.1007/s10549-009-0600-1.
18. Kim MS, Chang X, Yamashita K, Nagpal JK, Baek JH, Wu G, Trink B, Ratovitski EA, Mori M, Sidransky D, et al. Aberrant promoter methylation and tumor suppressive activity of the DFNA5 gene in colorectal carcinoma. Oncogene. 2008;27(25):3624–3634. doi: 10.1038/sj.onc.1211021.
19. Op De Beeck K, Van Laer L, Van Camp G. DFNA5, a gene involved in hearing loss and cancer: a review. Ann Otol Rhinol Laryngol. 2012;121(3):197–207. doi: 10.1177/000348941212100310.
20. Rogers C, Erkes DA, Nardone A, Aplin AE, Fernandes-Alnemri T, Alnemri ES. Gasdermin pores permeabilize mitochondria to augment caspase-3 activation during apoptosis and inflammasome activation. Nat Commun. 2019;10(1):1689–. doi: 10.1038/s41467-019-09397-2.
21. Zhang Z, Zhang Y, Xia S, Kong Q, Li S, Liu X, Junqueira C, Meza-Sosa KF, Mok TMY, Ansara J, et al. Gasdermin E suppresses tumour growth by activating anti-tumour immunity. Nature. 2020;579(7799):415–420. doi: 10.1038/s41586-020-2071-9.
22. Colaprico A, Silva TC, Olsen C, Garofano L, Cava C, Garolini D, Sabedot TS, Malta TM, Pagnotta SM, Castiglioni I, et al. Tcgabiolinks: an R/Bioconductor package for integrative analysis of TCGA data. Nucleic Acids Res. 2016;44(8):e71. doi: 10.1093/nar/gkv1507.
23. Mounir M, Lucchetta M, Silva TC, Olsen C, Bontempi G, Chen X, Noushmehr H, Colaprico A, Papaleo E. New functionalities in the TCGAbiolinks package for the study and integration of cancer data from GDC and GTEx. PLOS Comput Biol. 2019;15(3):e1006701. doi: 10.1371/journal.pcbi.1006701.
24. Chen Y, Lun AT, Smyth GK. From reads to genes to pathways: differential expression analysis of RNA-Seq experiments using rsubread and the edgeR quasi-likelihood pipeline. F1000 Res. 2016;5:1438. doi: 10.12688/f1000research.8987.2 .
25. Love MI, Huber W, Anders S. Moderated estimation of Fold change and dispersion for RNA-seq data with DESeq2. Genome Biology. 2014;15(12):550. doi: 10.1186/s13059-014-0550-8.
26. Robinson MD, McCarthy DJ, Smyth GK. edgeR: a Bioconductor package for differential expression analysis of digital gene expression data. Bioinformatics. 2010;26(1):139–140. doi: 10.1093/bioinformatics/btp616.
27. Erkes DA, Cai W, Sanchez IM, Purwin TJ, Rogers C, Field CO, Berger AC, Hartsough EJ, Rodeck U, Alnemri ES, et al. Mutant BRAF and MEK Inhibitors regulate the tumor immune microenvironment via pyroptosis. Cancer Discov. 2020;10(2):254–269. doi: 10.1158/2159-8290.CD-19-0672.
28. Kanehisa M, Goto S. KEGG: kyoto encyclopedia of genes and genomes. Nucleic Acids Res. 2000;28(1):27–30.
29. Hänzelmann S, Castelo R, Guinney J. GSVA: gene set variation analysis for microarray and RNA-seq data. BMC Bioinf. 2013;14(1):7. doi: 10.1186/1471-2105-14-7.
30. Enot DP, Vacchelli E, Jacquelot N, Zitvogel L, Kroemer G. TumGrowth: an open-access web tool for the statistical analysis of tumor growth curves. Oncoimmunology. 2018;7(9):e1462431. doi: 10.1080/2162402X.2018.1462431.
31. Campbell KM, Amouzgar M, Pfeiffer SM, Howes TR, Medina E, Travers M, Steiner G, Weber JS, Wolchok JD, Larkin J, et al. Prior anti-CTLA-4 therapy impacts molecular characteristics associated with anti-PD-1 response in advanced melanoma. Cancer Cell. 2023;41(4):791–806.e4. doi: 10.1016/j.ccell.2023.03.010.
32. Zhang Z, Zhang Y, Xia S, Kong Q, Li S, Liu X, Junqueira C, Meza-Sosa KF, Mok TMY, Ansara J, et al. Gasdermin E suppresses tumour growth by activating anti-tumour immunity. Nature. 2020;579(7799):415–420. doi: 10.1038/s41586-020-2071-9.
33. Koerner J, Horvath D, Herrmann VL, MacKerracher A, Gander B, Yagita H, Rohayem J, Groettrup M. PLGA-particle vaccine carrying TLR3/RIG-I ligand riboxxim synergizes with immune checkpoint blockade for effective anti-cancer immunotherapy. Nat Commun. 2021;12(1):2935. doi: 10.1038/s41467-021-23244-3.
34. Lutz J, Meister M, Habbeddine M, Fiedler K, Kowalczyk A, Heidenreich R. Local immunotherapy with the RNA-based immune stimulator CV8102 induces substantial anti-tumor responses and enhances checkpoint inhibitor activity. Cancer Immunol, Immunother: CII. 2023;72(5):1075–1087. doi: 10.1007/s00262-022-03311-4.
35. Böttcher JP, Reis E, Sousa C. The role of type 1 conventional dendritic cells in cancer immunity. Trends Cancer. 2018;4(11):784–792. doi: 10.1016/j.trecan.2018.09.001.
36. De Schutter E, Croes L, Ibrahim J, Pauwels P, Op de Beeck K, Vandenabeele P, Van Camp G. GSDME and its role in cancer: from behind the scenes to the front of the stage. Int J Cancer. 2021;148(12):2872–2883. doi: 10.1002/ijc.33390.
37. Akbani R, Akdemir K, Aksoy B, Albert M, Ally A, Amin S, Arachchi H, Arora A, Auman J, Ayala B, et al. Genomic classification of cutaneous melanoma. Cell. 2015;161(7):1681–1696. doi: 10.1016/j.cell.2015.05.044.
38. Morrison C, Pabla S, Conroy JM, Nesline MK, Glenn ST, Dressman D, Papanicolau-Sengos A, Burgher B, Andreas J, Giamo V, et al. Predicting response to checkpoint inhibitors in melanoma beyond PD-L1 and mutational burden. J For Immunother Of Cancer. 2018;6(1):32. doi: 10.1186/s40425-018-0344-8.
39. Chiappinelli KB, Strissel PL, Desrichard A, Li H, Henke C, Akman B, Hein A, Rote N, Cope L, Snyder A, et al. Inhibiting DNA methylation causes an interferon response in cancer via dsRNA including endogenous retroviruses. Cell. 2015;162(5):974–986. doi: 10.1016/j.cell.2015.07.011.
40. Gide TN, Quek C, Menzies AM, Tasker AT, Shang P, Holst J, Madore J, Lim SY, Velickovic R, Wongchenko M, et al. Distinct immune cell populations define response to anti-PD-1 monotherapy and anti-PD-1/Anti-CTLA-4 combined therapy. Cancer Cell. 2019;35(2):238–55.e6. doi: 10.1016/j.ccell.2019.01.003.
41. Wang Y-Y, Wang J, Wang S, Yang Q-C, Song A, Zhang M-J, Wang W-D, Liu Y-T, Zhang J, Wang W-M, et al. Dual-responsive epigenetic inhibitor Nanoprodrug combined with oncolytic virus synergistically boost cancer immunotherapy by igniting gasdermin E-Mediated pyroptosis. ACS Nano. 2024;18(31):20167–20180. doi: 10.1021/acsnano.4c03034.
42. Lu Y, He W, Huang X, He Y, Gou X, Liu X, Hu Z, Xu W, Rahman K, Li S, et al. Strategies to package recombinant Adeno-associated virus expressing the N-terminal gasdermin domain for tumor treatment. Nat Commun. 2021;12(1):7155. doi: 10.1038/s41467-021-27407-0.
43. Cullen JK, Yap PY, Ferguson B, Bruce ZC, Koyama M, Handoko H, Hendrawan K, Simmons JL, Brooks KM, Johns J, et al. Tigilanol tiglate is an oncolytic small molecule that induces immunogenic cell death and enhances the response of both target and non-injected tumors to immune checkpoint blockade. J For

Immunother Of Cancer. 2024;12(4):12. doi: 10.1136/jitc-2022-006602.
44. Wang Q, Wang Y, Ding J, Wang C, Zhou X, Gao W, Huang H, Shao F, Liu Z. A bioorthogonal system reveals antitumour immune function of pyroptosis. Nature. 2020;579(7799):421–426. doi: 10.1038/s41586-020-2079-1.
45. Zhou Z, He H, Wang K, Shi X, Wang Y, Su Y, Wang Y, Li D, Liu W, Zhang Y, et al. Granzyme a from cytotoxic lymphocytes cleaves GSDMB to trigger pyroptosis in target cells. Science. 2020;368(6494). doi: 10.1126/science.aaz7548.
46. Hou J, Zhao R, Xia W, Chang CW, You Y, Hsu JM, Nie L, Chen Y, Wang Y-C, Liu C, et al. PD-L1-mediated gasdermin C expression switches apoptosis to pyroptosis in cancer cells and facilitates tumour necrosis. Nat Cell Biol. 2020;22(10):1264–1275. doi: 10.1038/s41556-020-0575-z.
47. Schadt L, Sparano C, Schweiger NA, Silina K, Cecconi V, Lucchiari G, Yagita H, Guggisberg E, Saba S, Nascakova Z, et al. Cancer-cell-intrinsic cGAS expression mediates tumor immunogenicity. Cell Rep. 2019;29(5):1236–48.e7. doi: 10.1016/j.celrep.2019.09.065.
48. Zhao Z, Li Q, Ashraf U, Yang M, Zhu W, Gu J, Chen Z, Gu C, Si Y, Cao S, et al. Zika virus causes placental pyroptosis and associated adverse fetal outcomes by activating GSDME. eLife. 2022;11:e73792. doi: 10.7554/eLife.73792.
49. Showalter A, Limaye A, Oyer JL, Igarashi R, Kittipatarin C, Copik AJ, Khaled AR. Cytokines in immunogenic cell death: applications for cancer immunotherapy. Cytokine. 2017;97:123–132. doi: 10.1016/j.cyto.2017.05.024.
50. Chow MT, Ozga AJ, Servis RL, Frederick DT, Lo JA, Fisher DE, Freeman GJ, Boland GM, Luster AD. Intratumoral activity of the CXCR3 Chemokine system is required for the efficacy of anti-PD-1 therapy. Immunity. 2019;50(6):1498–512.e5. doi: 10.1016/j.immuni.2019.04.010.
51. Van Hoecke L, Van Lint S, Roose K, Van Parys A, Vandenabeele P, Grooten J, Tavernier J, De Koker S, Saelens X. Treatment with mRNA coding for the necroptosis mediator MLKL induces antitumor immunity directed against neo-epitopes. Nat Commun. 2018;9(1):3417. doi: 10.1038/s41467-018-05979-8.
52. Snyder AG, Hubbard NW, Messmer MN, Kofman SB, Hagan CE, Orozco SL, Chiang K, Daniels BP, Baker D, Oberst A, et al. Intratumoral activation of the necroptotic pathway components RIPK1 and RIPK3 potentiates antitumor immunity. Sci Immunol. 2019;4(36):4. doi: 10.1126/sciimmunol.aaw2004.
53. Liu J, Hong M, Li Y, Chen D, Wu Y, Hu Y. Programmed cell death tunes tumor immunity. Front Immunol. 2022;13:847345. doi: 10.3389/fimmu.2022.847345.
54. Karki R, Sundaram B, Sharma BR, Lee S, Malireddi RKS, Nguyen LN, Christgen S, Zheng M, Wang Y, Samir P, et al. ADAR1 restricts ZBP1-mediated immune response and PANoptosis to promote tumorigenesis. Cell Rep. 2021;37(3):109858. doi: 10.1016/j.celrep.2021.109858.